METAGENOMIC NEXT-GENERATION SEQUENCING REVEALS MIAMIENSIS AVIDUS (CILIOPHORA: SCUTICOCILIATIDA) IN THE 2017 EPIZOOTIC OF LEOPARD SHARKS (TRIAKIS SEMIFASCIATA) IN SAN FRANCISCO BAY, CALIFORNIA, USA

Authors: Retallack, Hanna, Okihiro, Mark S., Britton, Elliot, Sommeran, Sean Van, and DeRisi, Joseph L.

Source: Journal of Wildlife Diseases, 55(2) : 375-386

Published By: Wildlife Disease Association

URL: https://doi.org/10.7589/2018-04-097

DOI: 10.7589/2018-04-097

Journal of Wildlife Diseases, 55(2), 2019, pp. 375–386

METAGENOMIC NEXT-GENERATION SEQUENCING REVEALS *MIAMIENSIS AVIDUS* (CILIOPHORA: SCUTICOCILIATIDA) IN THE 2017 EPIZOOTIC OF LEOPARD SHARKS (*TRIAKIS SEMIFASCIATA*) IN SAN FRANCISCO BAY, CALIFORNIA, USA

Hanna Retallack,[1] Mark S. Okihiro,[2,6] Elliot Britton,[3] Sean Van Sommeran,[4] and Joseph L. DeRisi[1,5]

[1] Department of Biochemistry and Biophysics, University of California San Francisco, 1700 4th St., San Francisco, California 94158, USA
[2] Fisheries Branch, Wildlife and Fisheries Division, California Department of Fish and Wildlife, 1880 Timber Trail, Vista, California 92081, USA
[3] San Francisco University High School, 3065 Jackson St., San Francisco, California 94115, USA
[4] Pelagic Shark Research Foundation, 750 Bay Ave. #2108, Capitola, California 95010, USA
[5] Chan Zuckerberg Biohub, 499 Illinois St., San Francisco, California 94158, USA
[6] Corresponding author (email: Mark.Okihiro@wildlife.ca.gov)

ABSTRACT: During March to August of 2017, hundreds of leopard sharks (*Triakis semifasciata*) stranded and died on the shores of San Francisco Bay, California, US. Similar mass stranding events occurred in 1967 and 2011, but analysis of those epizootics was incomplete, and no etiology was confirmed. Our investigation of the 2017 epizootic revealed severe meningoencephalitis in stranded sharks, raising suspicion for infection. We pursued a strategy for unbiased pathogen detection using metagenomic next-generation sequencing followed by orthogonal validation and further screening. We showed that the ciliated protozoan pathogen, *Miamiensis avidus*, was present in the central nervous system of leopard (n=12) and other shark species (n=2) that stranded in San Francisco Bay but was absent in leopard sharks caught elsewhere. This ciliated protozoan has been implicated in devastating outbreaks in teleost marine fish but not in wild elasmobranchs. Our results highlight the benefits of adopting unbiased metagenomic sequencing in the study of wildlife health and disease.

Key words: Epizootic, leopard shark, meningoencephalitis, metagenomic next-generation sequencing, *Miamiensis avidus*, San Francisco Bay, scuticociliate, *Triakis semifasciata*.

INTRODUCTION

The investigation of mass mortality events among wildlife populations can provide insight into ecosystem health and human impact. However, identifying an etiology is often challenging. Metagenomic next-generation sequencing (mNGS) provides an unbiased approach that has been used successfully in human and animal infections (Wilson et al. 2014; Zylberberg et al. 2016; Dervas et al. 2017). Through the analysis of all nucleic acids in a sample, mNGS can simultaneously test for all known organisms and can also identify novel pathogens, including distantly related species. Furthermore, the cost of NGS technologies continues to decrease, making these methods an increasingly viable option for routine wildlife surveillance and disease investigations.

In the past 50 years, several mass mortality events of unknown etiology have affected leopard sharks (*Triakis semifasciata*) in San Francisco (SF) Bay, California, US. In 1967, over 1,000 dead sharks, mainly leopard sharks, were collected in 1 mo in Alameda, California (Russo and Herald 1968; Russo 2015). More recently, unusual shark deaths were noted in the spring of 2006, and mass mortality again afflicted SF Bay leopard sharks in the spring and early summer of 2011, involving likely hundreds of leopard sharks, although the event was not systematically documented. Moribund sharks were often described as confused and disoriented, with erratic behaviors and swimming patterns.

Scuticociliates are free-living marine protozoa that belong to the subclass Scuticociliatida of the phylum Ciliophora (Gao et al. 2016). As opportunistic pathogens, several species of

scuticociliates have been reported to cause disease in diverse marine teleost fish species (Munday et al. 1997; Ramos et al. 2007; Garza et al. 2017) and, recently, in the subclass of cartilaginous fish known as elasmobranchs (Stidworthy et al. 2014; Li et al. 2017). Scuticociliatosis is an economically important problem for commercial marine fish culture (Iglesias et al. 2001) but has not been observed in wild fish populations.

We sought to identify a cause for mass mortality of leopard sharks in SF Bay in the spring of 2017. Using mNGS and confirmatory molecular and histologic assays, we identified the scuticociliate *Miamiensis avidus* in the central nervous system of stranded sharks, suggesting that this pathogen could contribute to significant disease in wild elasmobranchs.

MATERIALS AND METHODS

Shark stranding surveillance

The majority of shark and ray strandings were reported to the California Department of Fish and Wildlife (CDFW) by members of the public, often via The Marine Mammal Center (Sausalito, California) and the Pelagic Shark Research Foundation (Santa Cruz, California). Additional stranding data were provided by East Bay Regional Park District rangers (Oakland, California), the National Parks Service, and CDFW wardens working in and around San Francisco Bay. Stranding data were also acquired during three brief foot surveys of the Foster City, California, shoreline conducted by CDFW in April, June, and August 2017. Stranding data included date, location, species, approximate size, condition (live, dead, autolyzed), and presence of abnormal behavior (e.g., swimming in circles). Photos were often submitted, with occasional videos. Stranding data were recorded and sorted on the basis of species and date.

Sample collection

Stranded sharks were chosen for postmortem examination by a CDFW pathologist based on condition, with preference given to live moribund and fresh dead sharks (nonautolyzed with red gills). Sharks were either examined in the field or iced and examined postmortem at CDFW (Vista, California) within 72 h. Heads of some sharks were removed and frozen at –10 C until postmortem examination. Two captive sharks were examined: one Pacific angelshark (*Squatina californica*) on display at the Aquarium of the Bay (San Francisco, California), and one moribund leopard shark on display at the Marine Science Institute (Redwood City, California). As controls, grossly normal leopard sharks were collected by gill net from Newport Bay in southern California. A great white shark (*Carcharodon carcharias*) and soupfin shark (*Galeorhinus galeus*) were collected from outside SF Bay.

Postmortem examination

Sampled sharks were cleaned of external mud and debris with a freshwater spray. Species and sex were determined by examination of fins and dentition. Sharks were weighed, and total and fork length were measured. The dorsum of the head was cleaned with multiple passes using disposable disinfecting wipes (Clorox, Oakland, California, USA). When possible, endolymphatic pores were identified. The endolymphatic fossa (oval concave depression in the chondrocranium) was located by digital palpation. Using sterilized instruments, a 3×5-cm opening was made centered on the endolymphatic fossa and pores. Subcutaneous tissues overlying the fossa were sampled with a sterile cotton swab for microbiologic assessment. Subcutaneous fluid was aspirated with a sterile 1-mL pipette for cytologic assessment. The skin sample containing the endolymphatic pores and ducts was fixed in 10% formalin. The calvarium, including the endolymphatic fossa, was removed with a sterile scalpel and new blade then fixed in formalin. Removal of the calvarium exposed both inner ears and the cerebellum. Cerebrospinal fluid (CSF) overlying the cerebellum was sampled with a sterile cotton swab. Two 1-mL CSF samples were taken by sterile pipette and frozen at –10 C in cryovials. A third CSF sample was taken for cytologic assessment. Perilymph from one inner ear was sampled with a sterile cotton swab. A second perilymph sample was taken for cytologic assessment. The brain and olfactory lamellae were exposed by sharp dissection. The meninges, CSF, brain, inner ears, and olfactory lamellae were examined for evidence of inflammation and hemorrhage. Brains were separated from the chondrocranium by inversion of the skull and severing the cranial nerves. Olfactory lamellae and associated olfactory bulbs were removed by sharp dissection. The brain and olfactory lamellae were fixed in 10% formalin. In some sharks, one otic capsule was also taken and fixed in formalin. Gills, heart, kidneys, and abdominal organs were also examined postmortem. Selected organs were sampled and fixed in formalin from some sharks.

Cytology and histology

Samples of subcutaneous fluid surrounding the endolymphatic ducts, inner ear perilymph, and CSF were examined on glass slides under darkfield light microscopy at 200× and 400× with a binocular microscope. Red blood cells, inflammatory cells, and microbial pathogens were identified. Histology samples (primarily brain and nasal olfactory lamellae) were immersion-fixed in 10% formalin for 2 wk to 3 mo and then routinely paraffin-processed. Paraffin blocks were sectioned at 5–7 μm, and sections were stained with H&E, then examined with light microscopy. Degree of inflammation and necrosis, as well as numbers of protozoa in tissue sections, were semiquantitatively scored as not present (0), mild (1+), moderate (2+), or severe (3+).

Microbiology

Samples of subcutaneous fluid surrounding the endolymphatic ducts, inner ear perilymph, and CSF were plated onto blood agar and Sabouraud dextrose agar. Cultures were incubated aerobically at room temperature (15–20 C) for 4 wk and checked daily for growth. Selected isolates were sent to the University of Florida (Gainesville, Florida) for biochemical and PCR identification.

Nucleic acid extraction and sequencing

For RNA, 250 μL of CSF was placed in TRI-Reagent (Zymo Research, Irvine, California, USA) and homogenized with 2.8 mm ceramic beads (Omni, Kennesaw, Georgia, USA) on a TissueLyser II (Qiagen, Germantown, Maryland, USA) at 15 Hz for two 30-sec pulses, separated by 1 min on ice. Total RNA was then extracted using the Direct-zol RNA MicroPrep Kit with DNase treatment (Zymo Research) eluted in 12 μL and stored at –80 C until use. For DNA, 250 μL of CSF was placed in 750-μL lysis solution of the Fungal/Bacterial DNA Kit (Zymo Research) and homogenized as above with a single 2-min homogenization pulse. Total DNA was then extracted using the Fungal/Bacterial DNA Kit, eluted in 25 μL, and stored at –80 C until use. RNA samples were processed using 5 μL total RNA as input into the NEBNext Ultra II RNA Library Prep Kit for Illumina (New England Biolabs, Ipswich, Massachusetts, USA). Samples were sequenced on an Illumina MiSeq instrument using 150-nucleotide (nt) paired-end sequencing. A no-template control (nucleic acid–free water) was included in each batch of nucleic acid extractions and library preparation. Raw sequencing reads were deposited at the National Center for Biotechnology Information (NCBI) Sequence Read Archive under BioProject PRJNA438541, accession number SRP136047.

Primers used to amplify ciliate and shark genomic sequences are listed in Supplementary Material Table S1. Purified PCR products were sequenced by Quintarabio (Albany, California, USA) using the Sanger method (see Supplementary Material, Methods section).

Bioinformatics

Next-generation sequencing data were analyzed using a computational pipeline originally developed to identify potential pathogens in human samples (Wilson et al. 2014). Briefly, host sequences were identified with publicly available shark genomes and transcriptomes, and the remaining non–host sequences were compared with the NCBI nucleotide and protein databases. Potential pathogens were identified on the basis of a minimum read abundance, likelihood of pathogenicity, and absence in negative control samples. For species determination, reads mapping to the ciliate 18S small subunit (SSU) and 28S large subunit (LSU) of the nuclear ribosomal RNA locus (rRNA) were assembled and compared with the NCBI database by BLASTn (Altschul et al. 1990; NCBI 2018; see Supplementary Methods for details).

New sequences in this study were deposited in GenBank (accession nos. MH078243–MH078249, MH062876, MH064355) and include partial sequences of the mitochondrial cytochrome *c* oxidase I (*cox1*) gene, and SSU and LSU rRNA of the ciliate identified in the shark samples (see Supplementary Methods).

RESULTS

Beginning in March 2017, members of the public reported sharks swimming with unusual behaviors and stranding on beaches along the SF Bay shoreline, with the majority of strandings occurring in the Foster City area (Fig. 1). Leopard sharks were observed swimming unusually close to shore, appearing uncoordinated and disoriented, suggestive of an inner ear or central nervous system issue. At the height of the epizootic in April and May, 20–30 dead leopard sharks were being found daily along the shoreline in Foster City. We estimated that more than 1,000 leopard sharks died between March and August 2017 in SF Bay.

Postmortem examinations were performed on 11 fresh dead or live moribund leopard

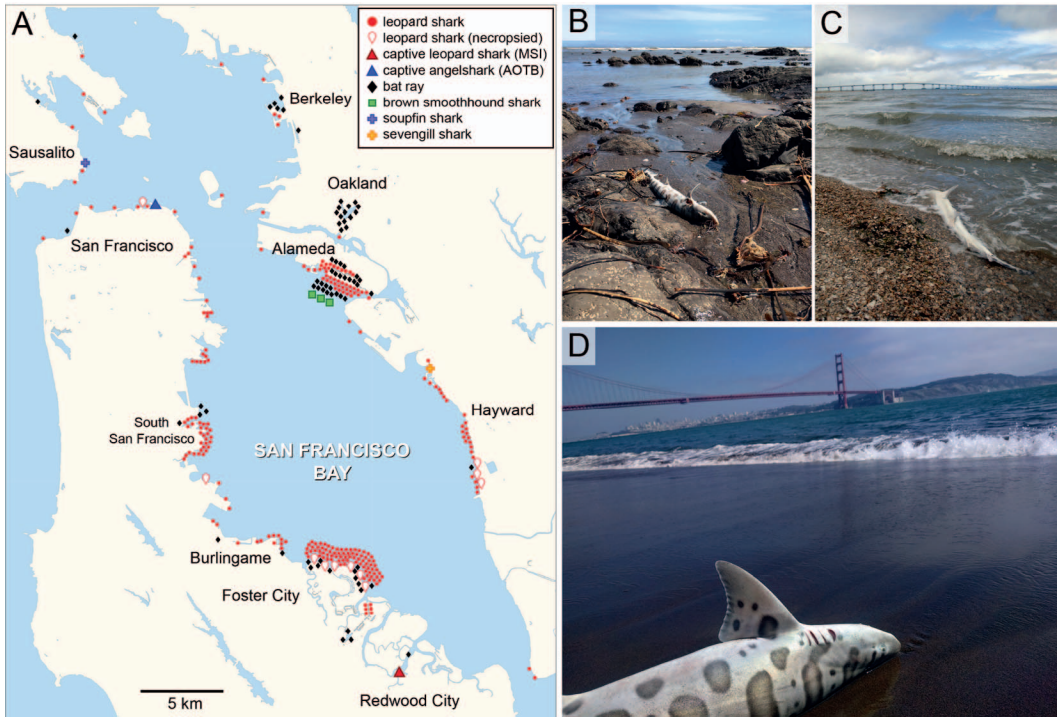

FIGURE 1. Map and photographs of shark strandings occurring in San Francisco Bay (SF Bay), California, USA in the spring of 2017. (A) Map of SF Bay showing locations of stranded sharks and bat rays, including leopard sharks (*Triakis semifasciata*), a Pacific angelshark (*Squatina californica*), bat rays (*Myliobatis californica*), brown smoothhound sharks (*Mustelus henlei*), a soupfin shark (*Galeorhinus galeus*), and a sevengill shark (*Notorynchus cepedianus*). MSI=Marine Science Institute; AOTB=Aquarium of the Bay. (B–D) Representative photographs of stranded leopard sharks around SF Bay taken between March and August 2017.

sharks, and on the heads of five frozen sharks. Gross and cytologic lesions were consistent with meningoencephalitis and were characterized by hemorrhage, cloudy CSF, and thickened meninges (Fig. 2). Lesions were especially prominent in the olfactory bulbs and lobes. Olfactory lamellae, adjacent to olfactory bulbs, were often markedly hemorrhagic and inflamed. There was no gross evidence of inflammation in the subcutaneous tissues surrounding the endolymphatic ducts or inner ears, which are target organs for a common bacterial pathogen, *Carnobacterium maltaromaticum*, of sharks (Schaffer et al. 2013). No lesions were observed in gills, heart, or abdominal organs. Cytologic examination of CSF revealed dense, mixed inflammation (mononuclear inflammatory cells and polymorphonuclear cells). No pathogens were observed. Conventional microbiology was uninformative: blood and Sabouraud dextrose agar cultures of CSF, inner ear perilymph, and subcutaneous tissues and surrounding endolymphatic ducts yielded no growth or fungal or bacterial contaminants associated with field sampling or postmortem colonization of tissues.

Guided by the signs of meningoencephalitis, samples of CSF were taken for molecular analysis from 15 stranded or ill-appearing sharks from SF Bay, including 11 leopard sharks, one sevengill shark (*Notorynchus cepedianus*), and one soupfin shark; one captive leopard shark from the Marine Science Institute; and one captive Pacific angelshark from the Aquarium of the Bay (Table 1; see also Supplementary Material Table S2). Control CSF samples were collected from four grossly normal leopard sharks captured by gill net from Newport Bay in

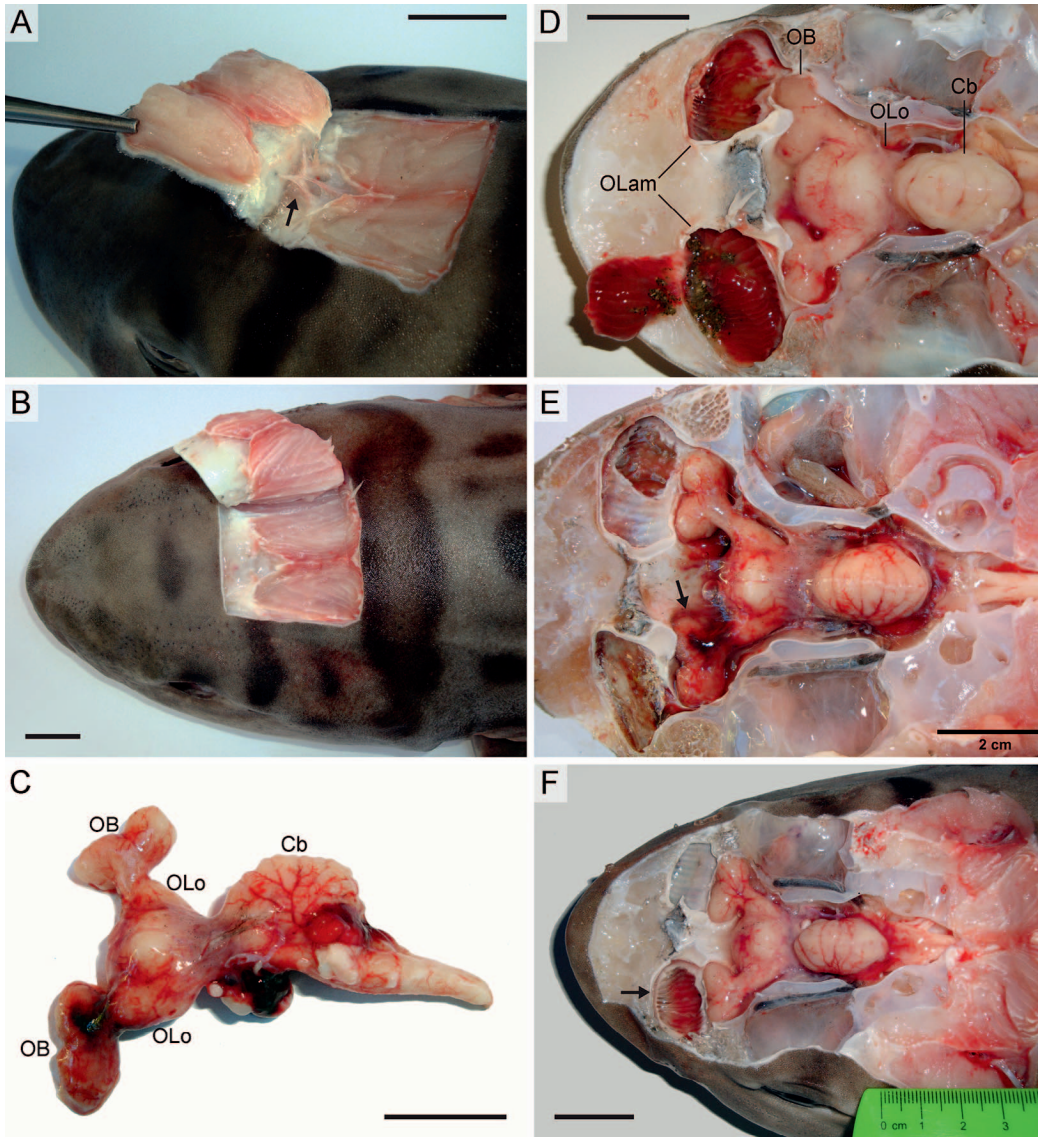

FIGURE 2. Gross observations of lesions in brains of stranded leopard sharks (*Triakis semifasciata*) in San Francisco Bay, California, USA in the spring of 2017 in which the scuticociliate *Miamiensis avidus* was involved. (A, B) Dissection from the superior aspect of the head exposing the endolymphatic ducts (arrow). (C) Brain with hemorrhagic lesions removed from cranial cavity of panel B and depicted in situ in panel E. (D–F) Dissection of cranial vault revealing superior surface of brain, hemorrhagic lesions, and congested olfactory lamellae (arrows). OB=olfactory bulb; OLo=olfactory lobe; Cb=cerebellum; OLam=olfactory lamellae. Scale bars=2 cm.

southern California and from two sharks with meningoencephalitis that had died in southern or central California: one great white shark and one soupfin shark.

To identify potential pathogens associated with leopard shark mortality, we performed mNGS on CSF samples from five sharks exposed to SF Bay water and two sharks from elsewhere on the California coast. Reads aligning to species in the Ciliophora phylum (taxonomy ID 5878) were identified in all five SF Bay sharks but were absent from the no-

TABLE 1. Summary of histologic findings and molecular diagnostics from stranded sharks from San Francisco Bay (LS01–12, S1–3) and control animals from central and southern California, USA (LS13–16, S4, S5). Sharks were sampled as part of an investigation of a large-scale mortality event of leopard sharks (*Triakis semifasciata*) in the San Francisco Bay area in March–August 2017. Species other than leopard sharks include Pacific angelshark (*Squatina californica*), sevengill shark (*Notorynchus cepedianus*), soupfin shark (*Galeorhinus galeus*), and great white shark (*Carcharodon carcharias*).[a]

Fish ID	Shark species	Collection		Histopathology		mNGS ciliate[c]	PCR *M. avidus*[d]
		Date	Location	Meningoencephalitis[b]	Protozoa		
LS01	*T. semifasciata*	9 April	San Francisco	Severe	Brain	n/a	+
LS02	*T. semifasciata*	15 April	Foster City	Severe	Brain	n/a	+
LS03	*T. semifasciata*	25 April	Foster City	Severe	–	n/a	+
LS04	*T. semifasciata*	25 April	Foster City	n/a	n/a	n/a	+
LS05	*T. semifasciata*	25 April	Hayward	n/a	n/a	n/a	+
LS06	*T. semifasciata*	25 April	Hayward	n/a	n/a	n/a	+
LS07	*T. semifasciata*	25 April	Hayward	n/a	n/a	n/a	+
LS08	*T. semifasciata*	26 April	Foster City	Severe	Brain/OL	+	+
LS09	*T. semifasciata*	26 April	Foster City	Severe	Brain	n/a	+
LS10	*T. semifasciata*	2 May	San Francisco	Severe	Brain/OL	+	+
LS11	*T. semifasciata*	13 May	Foster City	n/a	n/a	n/a	+
LS12	*T. semifasciata*[e]	23 May	MSI	Severe	Brain	+	+
S1	*S. californica*[e]	17 May	AOTB	Mild	–	+	+
S2	*N. cepedianus*	17 May	San Leandro	Severe	–	+	+
S3	*G. galeus*	5 July	Sausalito	Moderate	–	n/a	–
LS13	*T. semifasciata*	18 July	Newport Harbor	n/a	n/a	n/a	–
LS14	*T. semifasciata*	18 July	Newport Harbor	n/a	n/a	n/a	–
LS15	*T. semifasciata*	18 July	Newport Harbor	n/a	n/a	n/a	–
LS16	*T. semifasciata*	18 July	Newport Harbor	n/a	n/a	n/a	–
S4	*C. carcharias*	8 April	Santa Cruz	Severe	–	–	–
S5	*G. galeus*	24 May	La Jolla	Severe	–	–	–

[a] mNGS = metagenomic next-generation sequencing; – = absent/negative; + = present/positive; n/a = assay not performed (not applicable); OL = olfactory lamellae; MSI = Marine Science Institute (Redwood City, California); AOTB = Aquarium of the Bay (San Francisco, California).

[b] Meningoencephalitis in olfactory lamellae or brain (olfactory bulbs/lobes).

[c] Ciliate identified by mNGS.

[d] *Miamiensis avidus* identified by PCR.

[e] Captive shark on display in aquarium.

template control and non-SF Bay sharks (see Supplementary Material Table S3). No other credible pathogens were identified. Sixty-four percent of identified Ciliophora reads aligned to the ciliate rRNA locus. High-confidence contigs were assembled for the partial SSU (943 nt with a gap of 310 nt) and LSU (1916 nt with gaps of 39 and 56 nt) rRNA, with coverage between four and 2,545 unique reads and nucleotide identity >99%. The SSU contig aligned with greater confidence to *M. avidus* than other scuticociliate species by BLASTn.

To confirm mNGS results with an orthogonal molecular approach, we amplified a variable region of the ciliate *cox1* gene from DNA extracted from the CSF of these sharks. Amplification was detected in a nested PCR for *M. avidus* in five of five stranded sharks that were positive for *M. avidus* by mNGS (Fig. 3A; see Supplementary Material Fig. S1), and no amplification was detected in two of two sharks negative by mNGS or in the no-template control (see Supplementary Material Fig. S1). The sequence of the *cox1* amplicons (by the Sanger method) was most similar to other *M. avidus* sequences (Fig. 3B).

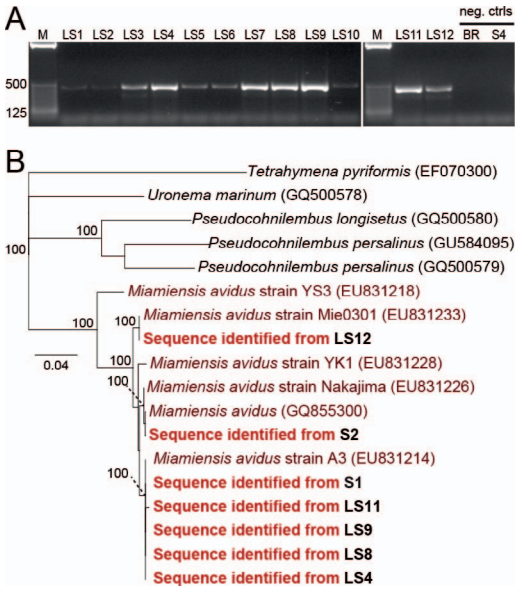

FIGURE 3. Molecular identification of the scuticociliate parasite *Miamiensis avidus* in cerebrospinal fluid from leopard sharks (*Triakis semifasciata*) in San Francisco Bay (SF Bay), California, USA in the spring of 2017. (A) DNA samples from SF Bay leopard sharks (LS1–12) and negative control animals (bat ray [BR] and S4) were tested by nested PCR using primers specific to the cytochrome *c* oxidase I (*cox*1) gene of *M. avidus* (expected size 422 bp). M: 25-bp ladder. (B) Neighbor-joining phylogenetic tree constructed from mitochondrial *cox1* nucleotide sequences. *Tetrahymena pyriformis* served as the outgroup. New sequences in this study are in bold, labeled according to fish ID (see Table 1). Nodes are labeled with bootstrap values based on 1,000 resamplings (for values >80). GenBank accession numbers provided for reference sequences. Scale bar=nucleotide substitutions per site.

Given these findings, brain and nasal tissues from nine affected sharks were more closely examined for histopathologic evidence of ciliated protozoa (Table 2). The majority of sharks examined histologically had moderate to severe inflammation and mild to severe necrosis in the olfactory lamellae of the nose (Fig. 4). Inflammation was variable in composition but was largely a mixed infiltrate of mononuclear cells (macrophages and lymphocytes) and polymorphonuclear cells (primarily eosinophils and heterophils). Lamellar inflammation was present within the hyperplastic mucosal epithelium, expanded submucosal connective tissues, and branches of the olfactory nerve. Ciliated protozoan parasites, morphologically consistent with *M. avidus*, were present in the olfactory lamellae of two sharks in small numbers. Protozoa were oblong, with irregular eccentric nuclei and characteristic vacuolated basophilic cytoplasm. Cytoplasmic vacuoles were clear or filled with pale eosinophilic material. Parasites were 20–30 μm in length by 10–20 μm wide.

In the brain, inflammatory and necrotizing lesions were concentrated rostrally in the meninges and parenchyma of the olfactory bulbs and olfactory lobes. Cellular composition of inflammatory lesions was comparable to that of lesions in the olfactory lamellae. Inflammatory lesions were consistently associated with moderate to marked congestion of capillaries and veins in the meninges and parenchyma of the brain. The majority of sharks also had severe congestion of blood vessels associated with the lateral ventricles of the olfactory bulbs and lobes. Many lateral ventricles were filled with mixed inflammatory cells. Necrotizing lesions were characterized by finely granular, pale, eosinophilic cellular debris mixed with degenerating and necrotic inflammatory cells, degenerating and necrotic neurons, and variable numbers of protozoa. Small to large numbers of protozoa were found in olfactory bulb or lobe sections of five of nine sharks. In many necrotic sections of brain, protozoa were present in large numbers but were often difficult to detect because of loss of membrane integrity and loss of cytoplasmic and nuclear basophilia. Necrotic protozoa could, however, usually be identified because of their relatively larger size and because of characteristic cytoplasmic vacuoles. Intact protozoa were similar to those observed in the olfactory lamellae. Caudally, inflammatory and necrotizing lesions were less common and less severe in the optic lobes and cerebellum, corresponding to fewer protozoa. Of the nine sharks examined, the captive angelshark (fish ID S1) had the fewest and mildest histologic lesions and no protozoa.

With evidence for *M. avidus* as a candidate pathogen, we used PCR to screen nine additional leopard sharks that stranded in SF Bay in the spring of 2017, compared with four

TABLE 2. Histopathologic lesions in stranded and captive sharks from San Francisco Bay, California, USA. Sharks were sampled as part of an investigation of a large-scale mortality event of leopard sharks (*Triakis semifasciata*) in the San Francisco Bay area in March–August 2017. Species other than leopard sharks include Pacific angelshark (*Squatina californica*) and sevengill shark (*Notorynchus cepedianus*). Tissues were examined for inflammation (I), necrosis (N), and abundance of protozoa (P) and scored on a four-point scale as not present (0), mild (1+), moderate (2+), or severe (3+).[a]

		Olfactory lamellae			Olfactory bulbs			Olfactory lobes			Optic lobes			Cerebellum		
Fish ID	Shark species	I	N	P	I	N	P	I	N	P	I	N	P	I	N	P
LS01	*T. semifasciata*	3+	1+	0	3+	3+	1+	2+	1+	0	0	0	0	1+	0	0
LS02	*T. semifasciata*	3+	0	0	3+	3+	0	3+	1+	0	3+	1+	1+	2+	0	0
LS03	*T. semifasciata*	n/a	n/a	n/a	3+	3+	0	3+	1+	0	3+	2+	0	1+	0	0
LS08	*T. semifasciata*	3+	3+	1+	3+	3+	2+	3+	3+	3+	1+	0	0	1+	0	0
LS09	*T. semifasciata*	3+	2+	0	3+	3+	0	3+	3+	2+	1+	0	0	n/a	n/a	n/a
LS10	*T. semifasciata*	2+	0	1+	3+	3+	3+	3+	3+	3+	2+	3+	3+	n/a	n/a	n/a
LS12	*T. semifasciata*	2+	1+	0	3+	3+	3+	3+	3+	3+	n/a	n/a	n/a	n/a	n/a	n/a
S1	*S. californica*	1+	0	0	1+	1+	0	0	0	0	0	0	0	0	0	0
S2	*N. cepedianus*	3+	1+	0	3+	3+	0	3+	2+	0	3+	2+	0	3+	2+	0

[a] n/a = not examined.

grossly normal leopard sharks that were caught in southern California. A soupfin shark that stranded in SF Bay in July 2017 was also tested. The PCR was targeted to the ciliate SSU and mitochondrial *cox1* regions, initially using universal ciliate primers (Jung et al. 2005; Whang et al. 2013), followed by Sanger sequencing or species-specific nested PCR for

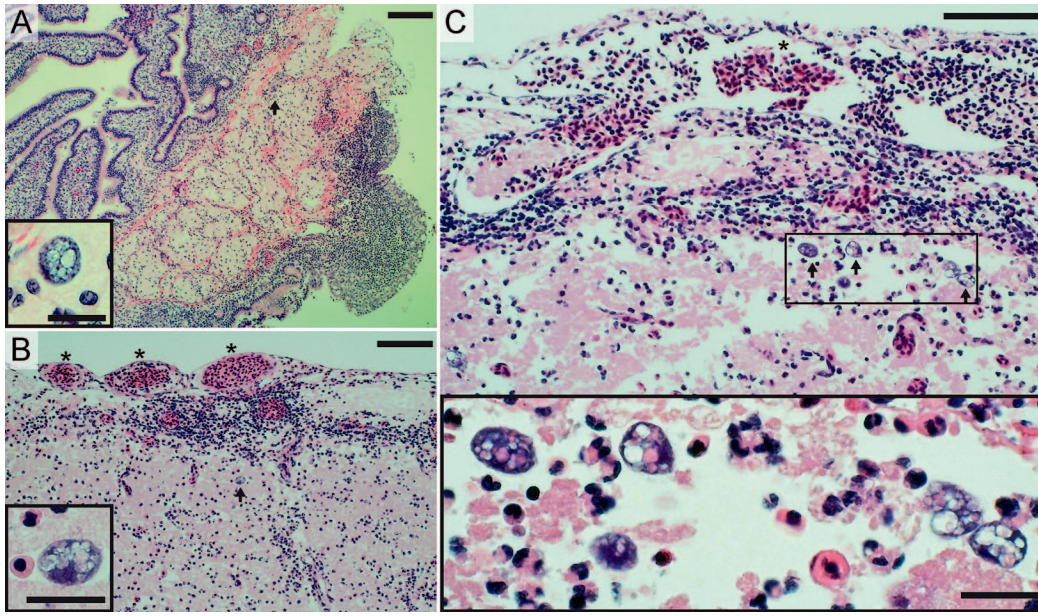

FIGURE 4. Histology showing protozoa morphologically consistent with the scuticociliate *Miamiensis avidus* in brain tissues of stranded leopard sharks in San Francisco Bay, California, USA in the spring of 2017. (A) Olfactory lamellae (top left) and filament (center), with submucosal inflammation (bottom right) and scattered protozoa (arrow, magnified in inset). Scale bar=200 μm (inset bar=25 μm). (B, C) Olfactory bulb of the brain with congested vessels in overlying meninges (asterisks), inflammatory infiltrate, and protozoa (arrows, magnified in insets). Scale bars=100 μm (inset bar=25 μm). Representative sections stained with H&E are shown.

the *cox1* gene to test for the related pathogenic ciliate species, *Uronema marinum*, *Pseudocohnilembus longsietus*, and *Pseudocohnilembus persalinus* (Whang et al. 2013). For *cox1*, amplification specific to *M. avidus* was detected in nine of nine SF Bay leopard sharks (Fig. 3A; see Supplementary Material Fig. S2), and was not detected in the southern California leopard sharks (see Supplementary Material Fig. S3) or the SF Bay soupfin shark (see Supplementary Material Fig. S1). Amplicon sequencing revealed 99.1% pairwise identity. The *cox1* sequences clustered together with reference *M. avidus* sequences on a neighbor-joining tree (Fig. 3B). For the SSU, an amplicon of the expected size was detected in three of 12 SF Bay leopard sharks and in the two SF Bay non–leopard sharks that were positive by mNGS and was absent from all four of the leopard sharks and both of the non–leopard sharks from southern California (see Supplementary Material Fig. S4). The sequences of the ciliate SSU amplicon from five sharks (fish IDs LS3, LS4, LS11, S1, and S2) were 100% identical, were concordant with the regions of overlap from mNGS, and clustered together with reference *M. avidus* sequences on a neighbor-joining tree (see Supplementary Material Fig. S5).

DISCUSSION

In this study, we described an epizootic of wild leopard sharks characterized by stranding behavior and meningoencephalitis, and we provided strong molecular and histologic evidence that implicated the ciliated protozoan *M. avidus* as the candidate pathogen associated with the 2017 SF Bay mass mortality event. We identified *M. avidus* through an unbiased, NGS-based approach, which has been used previously in investigations of a wide range of human and nonhuman infectious diseases.

The lack of a leopard shark genome presented a technical challenge; thus, we utilized sequences from related species. Despite being unable to identify all host sequences using our proxy-metagenome host sequences, we were still able to identify a plausible pathogen embedded in a large amount of unrelated and unidentified host sequence. Future contributions of shotgun sequencing data will improve our ability to identify sequences of unusual hosts, such as sharks, thereby improving our ability to detect novel pathogens. Among the species-specific regions flanked by conserved sequences, such as the commonly used ribosomal RNA (SSU and LSU) and *cox1* genes, we found that *cox1* was similar to SSU and better than LSU in discriminating between *M. avidus* and related pathogenic scuticociliates. This finding is consistent with reports of higher intraspecific variation of the *cox1* gene (Budiño et al. 2011; Jung et al. 2011). Nonetheless, using multiple genes for molecular phenotyping can add confidence, because discrepancies remain in the field about highly similar taxa, such as *M. avidus* and *Philasterides dicentrarchi* (Jung et al. 2011; De Felipe et al. 2017), with subspecies divisions likely yet to be realized (Gao et al. 2012).

We observed *M. avidus* only in sharks exposed to SF Bay water, including two wild-caught animals in captivity. The associated phenotype was consistent with other reports of ciliate infection of elasmobranchs notable for necrotizing meningoencephalitis (Stidworthy et al. 2014; Li et al. 2017). Given the distribution of protozoa observed on histopathology, pathogenesis in leopard sharks likely involves a nasal route, as suggested for other host species (Moustafa et al. 2010), with initial protozoal invasion of olfactory lamellae, followed by extension into the olfactory bulbs and lobes of the brain. Massive inflammation and severe encephalomalacia associated with *M. avidus* infection could account for the disorientation and abnormal behavior of sharks before stranding. Further support implicating *M. avidus* in these repeated mortality events comes from the postmortem examination of a single leopard shark that stranded in the 2011 SF Bay epizootic that showed extensive inflammation and an abundance of unicellular ciliated protozoa throughout the brain (Kubiski et al. 2011). We found no evidence of other pathogens that have

been reported in elasmobranchs near the Pacific coast of North America.

We cannot exclude the possibility that *M. avidus* was not the primary or sole driver of disease and mortality. Factors such as water temperature, salinity, toxins, or other pathogens could increase susceptibility to an opportunistic infection by *M. avidus* (Hopkins and Cech 2003; Carlisle and Starr 2009). In SF Bay, leopard sharks may be especially vulnerable each spring when they aggregate in large numbers in the warm shallow waters of bays and estuaries (Hight and Lowe 2007; Nosal et al. 2013), with greater exposure to runoff that may contain toxins or decreased salinity. Lower salinity has been associated with increased fish mortality in the context of scuticociliate infection (Takagishi et al. 2009), and with more rapid growth of *P. dicentrarchi* (synonymous with *M. avidus*) in vitro (Iglesias et al. 2003). Notably, heavy seasonal rainfall with runoff into the bay preceded each of the spring epizootics in 2006, 2011, and 2017 (Fig. 5; National Oceanographic and Atmospheric Administration National Centers for Environmental Information 2018). Although the specific conditions that led to the 2017 episode of scuticociliatosis are not fully known, it is worth noting that scuticociliates have frequently been observed in marine fish hatcheries, in addition to wild fish populations. It would be prudent to better understand interactions between farmed and wild fish to identify risks to both populations. Further studies are needed to clarify susceptibility factors and exposures, especially in the context of major urban centers where planned human development could prevent or mitigate the negative effects of human activity on wild marine fish.

Future investigations of mass mortality events should include *M. avidus* as a potential pathogen. We anticipate that the episode of scuticociliatosis in wild elasmobranchs described here is not an isolated event. As similar epizootics are uncovered through seasonal monitoring, future research is needed to describe the host-pathogen relationship and potential implications for nearby human populations. Although the only known ciliate

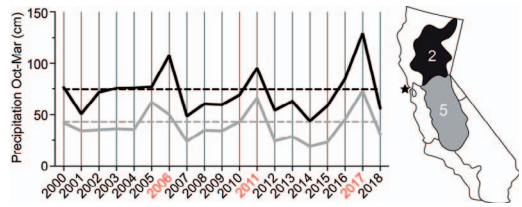

FIGURE 5. Precipitation in regions draining to San Francisco Bay (SF Bay), California, USA by year, including 2017 when strandings of leopard sharks (*Triakis semifasciata*) were associated with infection by *Miamiensis avidus*. Six-month cumulative precipitation (solid lines) ending in March of given year, in California Climate District 2 (Sacramento Drainage, black) and Climate District 5 (San Joaquin Drainage, gray). Mean October–March precipitation values for 1901–2000 plotted as baseline (dashed lines). Map of California (right) shows climate districts, respective to their outflow into SF Bay (star). Red highlights years with abnormal shark deaths in the spring. Precipitation data from National Oceanographic and Atmospheric Administration National Centers for Environmental Information.

parasite of humans, *Balantidium coli*, is far distantly related to scuticociliates (Schuster and Ramirez-Avila 2008) and no scuticociliates have been proven to cause pathogenic disease in mammals, sport fishing and consumption of leopard sharks is common in SF Bay, and the consequences of *M. avidus* ingestion are unknown. Finally, this study demonstrates the ability of mNGS to identify potential pathogens rapidly in an unbiased manner. Surveillance and disease investigations in wildlife populations will likely benefit from the incorporation of mNGS-based techniques.

ACKNOWLEDGMENTS

We acknowledge the Marine Science Institute (Redwood City, California), the Aquarium of the Bay (San Francisco, California), The Marine Mammal Center (Sausalito, California), East Bay Regional Park District (Oakland, California), and the National Parks Service for their assistance in this work. We also acknowledge Jennifer Kampe and Paige Coluccio for providing photos of stranded sharks, Maureen Anders for extensive field work on Alameda Island, and Eric Chow and Derek Bogdanoff at the Center for Advanced Technology (University of California San Francisco) for assistance with sequencing. This work was

supported by the Chan Zuckerberg Biohub (J.D.), UCSF Medical Scientist Training Program (H.R.), and the State of California (M.O.).

SUPPLEMENTARY MATERIAL

Supplementary material for this article is online at http://dx.doi.org/10.7589/2018-04-097.

LITERATURE CITED

Altschul SF, Gish W, Miller W, Myers EW, Lipman DJ. 1990. Basic local alignment search tool. *J Mol Biol* 215:403–410.

Budiño B, Lamas J, Pata MP, Arranz JA, Sanmartín ML, Leiro J. 2011. Intraspecific variability in several isolates of *Philasterides dicentrarchi* (syn. *Miamiensis avidus*), a scuticociliate parasite of farmed turbot. *Vet Parasitol* 175:260–272.

Carlisle AB, Starr RM. 2009. Habitat use, residency, and seasonal distribution of female leopard sharks *Triakis semifasciata* in Elkhorn Slough, California. *Mar Ecol Prog Ser* 380:213–228.

De Felipe AP, Lamas J, Sueiro RA, Folgueira I, Leiro JM. 2017. New data on flatfish scuticociliatosis reveal that *Miamiensis avidus* and *Philasterides dicentrarchi* are different species. *Parasitology* 144:1394–1411.

Dervas E, Hepojoki J, Laimbacher A, Romero-Palomo F, Jelinek C, Keller S, Smura T, Hepojoki S, Kipar A, Hetzel U. 2017. Nidovirus-associated proliferative pneumonia in the green tree python (*Morelia viridis*). *J Virol* doi: 10.1128/JVI.00718-17.

Gao F, Katz LA, Song W. 2012. Insights into the phylogenetic and taxonomy of philasterid ciliates (Protozoa, Ciliophora, Scuticociliatia) based on analyses of multiple molecular markers. *Mol Phylogenet Evol* 64:308–317.

Gao F, Warren A, Zhang Q, Gong J, Miao M, Sun P, Xu D, Huang J, Yi Z, Song W. 2016. The all-data-based evolutionary hypothesis of ciliated protists with a revised classification of the phylum Ciliophora (Eukaryota, Alveolata). *Sci Rep* 6:24874.

Garza JB, Bott NJ, Hammond MD, Shepherd N, Nowak BF. 2017. Molecular characterisation of *Miamiensis avidus* (Ciliophora: Scuticociliata) from ranched southern bluefin tuna, *Thunnus maccoyii* off Port Lincoln, South Australia. *Aquaculture* 469:44–49.

Hight BV, Lowe CG. 2007. Elevated body temperatures of adult female leopard sharks, *Triakis semifasciata*, while aggregating in shallow nearshore embayments: Evidence for behavioral thermoregulation? *J Exp Mar Biol Ecol* 352:114–128.

Hopkins TE, Cech JJ. 2003. The influence of environmental variables on the distribution and abundance of three elasmobranchs in Tomales Bay, California. *Environ Biol Fishes* 66:279–291.

Iglesias R, Paramá A, Álvareza MF, Leiro J, Aja C, Sanmartín ML. 2003. In vitro growth requirements for the fish pathogen *Philasterides dicentrarchi* (Ciliophora, Scuticociliatida). *Vet Parasitol* 111:19–30.

Iglesias R, Paramá A, Alvarez M, Leiro J, Fernández J, Sanmartín M. 2001. *Philasterides dicentrarchi* (Ciliophora, Scuticociliatida) as the causative agent of scuticociliatosis in farmed turbot *Scophthalmus maximus* in Galicia (NW Spain). *Dis Aquat Organ* 46:47–55.

Jung SJ, Im EY, Strüder-Kypke MC, Kitamura SI, Woo PTK. 2011. Small subunit ribosomal RNA and mitochondrial cytochrome *c* oxidase subunit 1 gene sequences of 21 strains of the parasitic scuticociliate *Miamiensis avidus* (Ciliophora, Scuticociliatia). *Parasitol Res* 108:1153–1161.

Jung SJ, Kitamura SI, Song JY, Joung IY, Oh MJ. 2005. Complete small subunit rRNA gene sequence of the scuticociliate *Miamiensis avidus* pathogenic to the flounder. *Dis Aquat Organ* 64:159–162.

Kubiski SV, Affolter VK, Groff J, Weber ES. 2011. *Pathology 11N1368 final report*. University of California Davis, Veterinary Medical Teaching Hospital, Davis, California, 2 pp.

Li WT, Lo C, Su CY, Kuo H, Lin SJ, Chang HW, Pang VF, Jeng CR. 2017. Locally extensive meningoencephalitis caused by *Miamiensis avidus* (syn. *Philasterides dicentrarchi*) in a zebra shark. *Dis Aquat Organ* 126:167–172.

Moustafa EMM, Tange N, Shimada A, Morita T. 2010. Experimental scuticociliatosis in Japanese flounder (*Paralichthys olivaceus*) infected with *Miamiensis avidus*: Pathological study on the possible neural routes of invasion and dissemination of the scuticociliate inside the fish body. *J Vet Med Sci* 72:1557–1563.

Munday B, O'Donoghue P, Watts M, Rough K, Hawkesford T. 1997. Fatal encephalitis due to the scuticociliate *Uronema nigricans* in sea-caged, southern bluefin tuna *Thunnus maccoyii*. *Dis Aquat Organ* 30:17–25.

NCBI (National Center for Biotechnology Information). 2018. *Basic local alignment search tool (BLAST)*. http://blast.ncbi.nlm.nih.gov/Blast.cgi. Accessed March 2018.

National Oceanographic and Atmospheric Administration National Centers for Environmental Information. 2018. *Climate at a glance: Divisional time series*. https://www.ncdc.noaa.gov/cag/divisional/time-series. Accessed March 2018.

Nosal AP, Cartamil DC, Long JW, Lührmann M, Wegner NC, Graham JB. 2013. Demography and movement patterns of leopard sharks (*Triakis semifasciata*) aggregating near the head of a submarine canyon along the open coast of southern California, USA. *Environ Biol Fishes* 96:865–878.

Ramos MF, Costa AR, Barandela T, Saraiva A, Rodrigues PN. 2007. Scuticociliate infection and pathology in cultured turbot *Scophthalmus maximus* from the north of Portugal. *Dis Aquat Organ* 74:249–253.

Russo RA. 2015. Observations of predation and loss among leopard sharks and brown smoothhounds in

San Francisco Bay, California. *Calif Fish Game* 101: 149–157.

Russo RA, Herald ES. 1968. The 1967 shark kill in San Francisco Bay. *Calif Fish Game* 54:215–216.

Schaffer PA, Lifland B, Van Sommeran S, Casper DR, Davis CR. 2013. Meningoencephalitis associated with *Carnobacterium maltaromaticum*–like bacteria in stranded juvenile salmon sharks (*Lamna ditropis*). *Vet Pathol* 50:412–417.

Schuster FL, Ramirez-Avila L. 2008. Current world status of *Balantidium coli*. *Clin Microbiol Rev* 21:626–638.

Stidworthy MF, Garner MM, Bradway DS, Westfall BD, Joseph B, Repetto S, Guglielmi E, Schmidt-Posthaus H, Thornton SM. 2014. Systemic scuticociliatosis (*Philasterides dicentrarchi*) in sharks. *Vet Pathol* 51: 628–632.

Takagishi N, Yoshinaga T, Ogawa K. 2009. Effect of hyposalinity on the infection and pathogenicity of *Miamiensis avidus* causing scuticociliatosis in olive flounder *Paralichthys olivaceus*. *Dis Aquat Organ* 86: 175–179.

Whang I, Kang H-SS, Lee J. 2013. Identification of scuticociliates (*Pseudocohnilembus persalinus*, *P. longisetus*, *Uronema marinum* and *Miamiensis avidus*) based on the cox1 sequence. *Parasitol Int* 62:7–13.

Wilson MR, Naccache SN, Samayoa E, Biagtan M, Bashir H, Yu G, Salamat SM, Somasekar S, Federman S, Miller S, et al. 2014. Actionable diagnosis of neuroleptospirosis by next-generation sequencing. *N Engl J Med* 370:2408–2417.

Zylberberg M, Van Hemert C, Dumbacher JP, Handel CM, Tihan T, DeRisi JL. 2016. Novel picornavirus associated with avian keratin disorder in Alaskan birds. *MBio* 7:e00874-16.

Submitted for publication 23 March 2018.
Accepted 28 July 2018.